

SOME EXPERIMENTAL EFFECTS ON THE CHARACTERISTIC
PHYSICAL PROPERTIES OF STEEL AS DETERMINED
BY X-RAY DIFFRACTION

A Thesis
Presented to
the Faculty of the School of Engineering
The University of Houston

In Partial Fulfillment
of the Requirements for the Degree
Master of Science in Mechanical Engineering

M. D. ANDERSON MEMORIAL LIBRARY
UNIVERSITY OF HOUSTON

by
John Elam Ashley

August 1956

158226

ACKNOWLEDGEMENTS

The author wishes to acknowledge the assistance and encouragement given him by Professor Leo J. Castellanos at the University of Houston. Acknowledgement is also given to Mr. Wiley B. Noble and the Reed Roller Bit Company, and to Mr. J. M. Williams, Jr. of the Reed Roller Bit Company, whose cooperation and interest made this work possible.

TABLE OF CONTENTS

INTRODUCTION	Page 1
RESUME OF X-RAY DIFFRACTION PRINCIPLES	Page 3
TECHNIQUE	Page 7
EXPERIMENTAL PROCEDURE	Page 10
First Investigation Relative to Measurement of Stress: "Preferred Orientation of Grinding Stresses".	
Second Investigation Relative to Measurement of Stress: "Preferred Orientation of Stresses from Extrusion".	
Third Investigation Relative to Measurement of Stress: "Temperature Effects".	
Fourth Investigation: "Comparison of Structure and Thermal Expansion Coefficient of 'Straight' Carbon Steels, Carburized Vs. Non-Carburized".	
SUMMARY AND CONCLUSIONS	Page 18
BIBLIOGRAPHY	Page 19
APPENDIX A. SAMPLE CALCULATIONS	Page 21
APPENDIX B. DATA TABLES	Page 24
APPENDIX C. POLE FIGURE DATA TABLE AND DIAGRAM	Page 27

LIST OF ILLUSTRATIONS

- Figure 1 - X-Rays Incident on and Reflected from the Specimen Surface
- Figure 2 - Diagramatic Sketch of Two Exposure Method
- Figure 3 - General View of General Electric XRD-3 X-Ray Diffraction Spectrogoniometer
- Figure 4 - X-Ray Pattern by Recorder of Hardened Steel
- Figure 5 - Graphic Sketch of (211) Martensite Peak
- Figure 6 - Pole Chart of Extruded Steel
- Figure 7 - Graph of the Stress Distribution After Grinding
- Figure 8 - Graph of the Stress Distribution After Extruding
- Figure 9 - View of XRD-3 X-Ray Diffraction Unit Set Up for Temperature Control

INTRODUCTION

Residual stress in steels and other metals has been a major concern of metallurgists and design engineers for many years. The definition for residual stress from the "Metals Handbook" (1, Page 12)* is given as follows: "Macroscopic stresses that are set up within a metal as the result of non-uniform plastic deformation. This deformation may be caused by cold working or by drastic gradients of temperature as from quenching or welding." It is obvious that the study of residual stresses is a paramount necessity, for its effects on the static and dynamic properties of finished parts might well be disastrous.

It is a well known fact in the field of heat treatment that complicated residual stress phenomena attend the quenching of steels from the austenitic state. Such quenching practice demands the foremost skill and experience to minimize distortion and prevent cracking. One might then consider these residual stresses as an evil by-product of a heat treatment designed to increase the physical properties of the finished piece were it not for the fact that residual stresses can contribute tremendously towards increasing the service life of countless parts manufactured from metal. Consequently, a knowledge of the magnitude and distribution of these forces and an ability to control them is essential to obtain the overall desired effect in the finished piece.

In an attempt to understand the origin of these "locked in stresses" and to learn of their influence, many techniques have been developed for their measurement. In general, these techniques are all destructive to the piece under study and do not permit a service test

*Number in parentheses refer to references in the Bibliography.

on the actual piece after the stresses have been evaluated.

The X-Ray technique, however, stands virtually alone in the field of non-destructive testing of residual stress. It is finding increasing application in industry, where for some problems, it offers conclusive advantages over the other systems. The X-Ray method detects elastic strain only, where as strain gages, for example, detect both elastic and plastic strains without distinction. The narrow X-Ray beam strikes an area about $1/4$ of a square inch which means that localized stresses and steep gradients can be studied. The X-Ray diffraction method measures only the superficial stresses, however, and in that regard only is it non-destructive. But, all other conditions being equal, the surface stress will define the sub-surface stress.

One big disadvantage is the initial cost. Compared to other methods, the expense is very high, even before special specimen rotating devices are included. As will be introduced later, many of the computations are tedious and time consuming; still another "price" to pay for accuracy and convenience.

Even with X-Ray diffraction man is still limited in the knowledge of internal stresses, for it is recognized that the X-Ray procedure, in common with all others, yields only an average macro-stress in the specimen and is in no way indicative of the micro-stresses present. If one might assume that a piece will fail from the micro-stresses alone, certainly a favorable macro-stress will minimize this influence. And, if we are ever to know the complete description, be it macro, micro, or both, surely we have a beginning here which very well might be the "key to the door".

RESUME' OF X-RAY DIFFRACTION PRINCIPLES

The principles of X-Ray diffraction have been known for a long time and are relatively simple. Prof. W. K. Rontgen discovered the X-Ray in 1895 while experimenting with highly evacuated cathode ray tubes at the University of Wurzburg, Germany. Later, M. Von Laue, then W. H. Bragg and his son W. L. Bragg in about 1915 used X-Rays in the solution of crystalline structures.

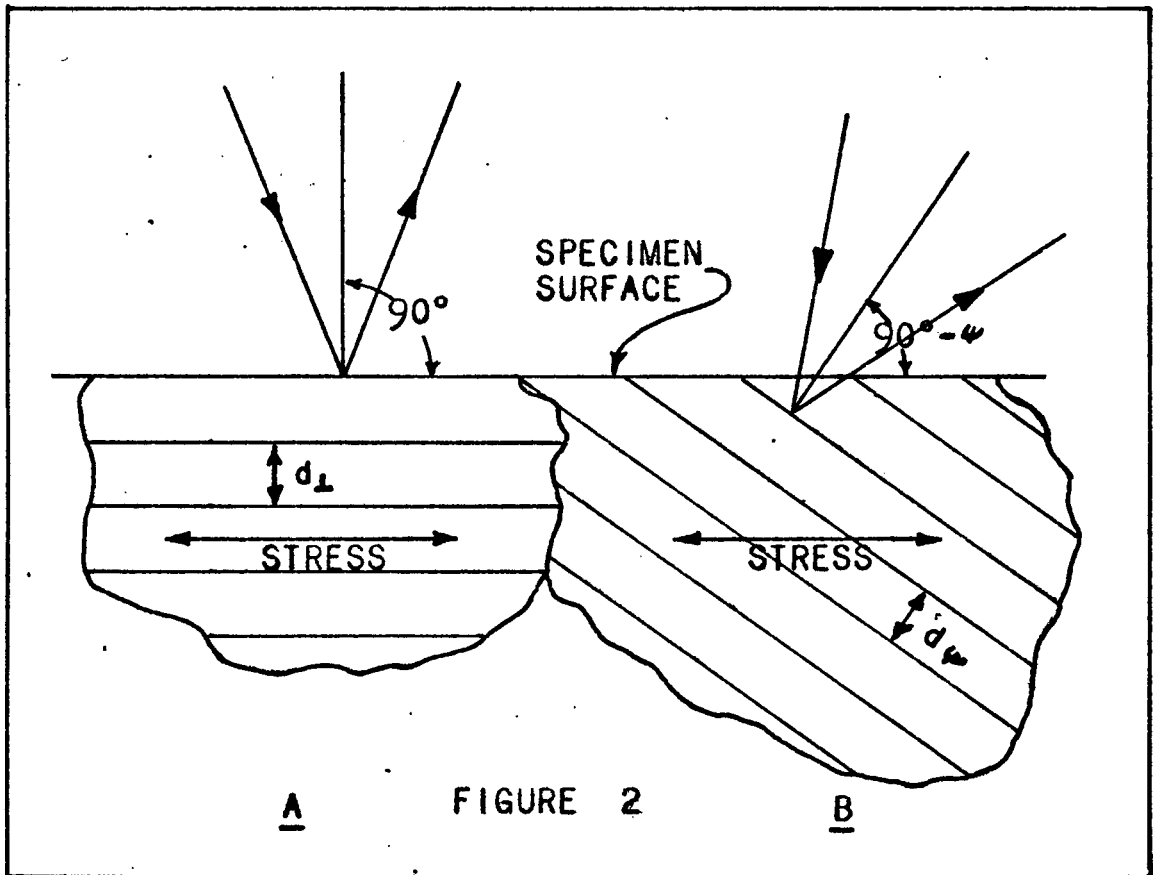
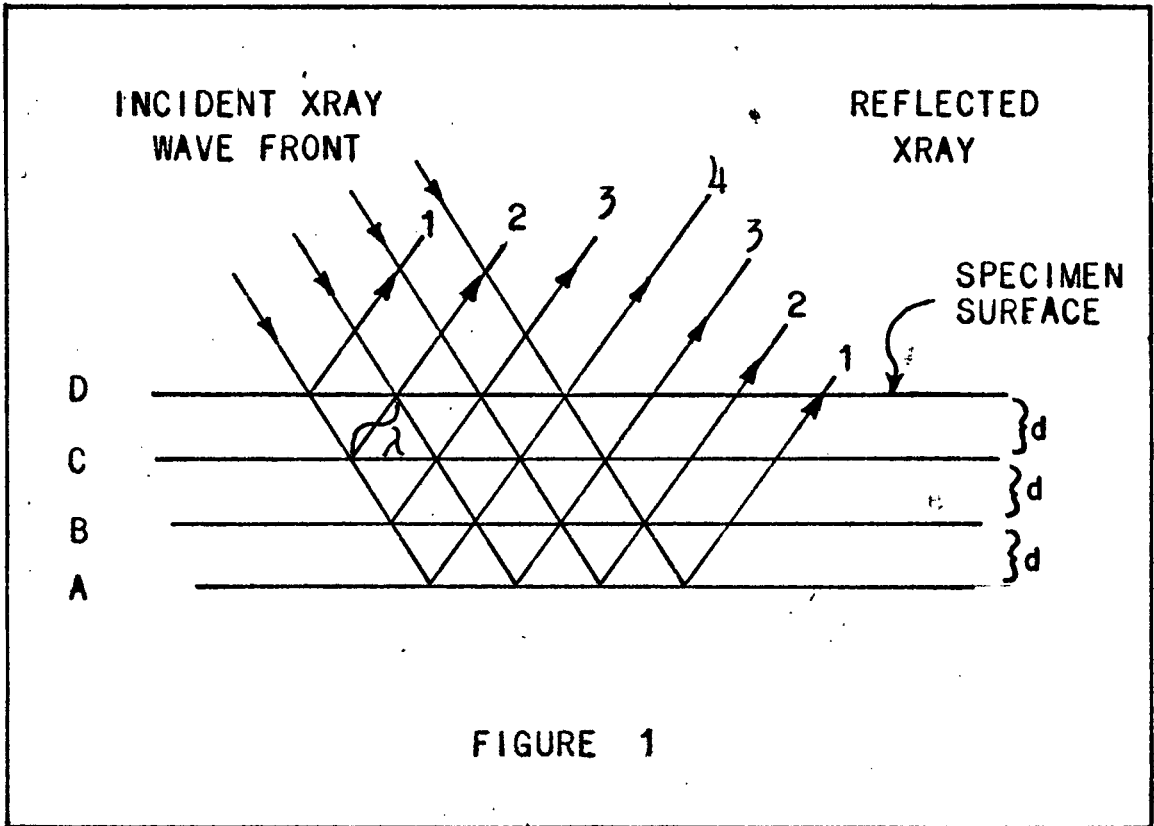
In the years 1925-26, H. H. Lester and R. H. Aborn (2) pioneered in the development of stress measurement, using X-Ray diffraction. It was shown that the interplanar spacing "d" between the atomic planes of the crystalline phase under study varied directly with the applied stress.

From Bragg's Law,

$$n \lambda = 2d \sin \theta, \quad (\text{Equation 1})$$

The "d" value can be determined for any measured value of the diffraction angle " θ ", where " λ " is the X-Ray wave length and "n" is a simple integer. Any change in "d" is a direct measure of strain, and from which the stress can be computed.

Let us consider just how the "d" value is calculated. An incident X-Ray wave front (Figure 1) strikes the surface of the specimen and reflects from the four atomic planes. The choice of four planes is merely for simplicity, as actually as many as one thousand planes are picked up, depending on the absorption coefficient of the material under study. As can be seen, the X-Ray beams tend to reinforce each other accumulating maximum intensity in the middle of the reflected beam. For other interplanar distances the angle of incidence θ



(theta) will have to be changed to bring about reinforcement again.

To observe this same set of planes with an X-Ray beam of shorter or longer wave length would also require a change to another angle of incidence. Only when the frequency is such that the wave fronts from successive planes are synchronized will reinforcement occur.

For every "d" and " λ " there is a corresponding angle θ since these parameters vary according to equation 1. Tables for conversion of diffraction angles to interplanar distances for several wave lengths can be purchased from the National Bureau of Standards, Applied Math Series, Government Printing Office.

One of the first methods of strain study following this procedure was developed by G. Sachs and J. Weertz (3) in 1930 and required a knowledge of the strain free interplanar distance. After determining this the specimen was stressed and a second measurement was made to determine the change in spacing from which the induced strain could be calculated. It appears that this method aside from its accuracy, was not much of an improvement over other methods in general.

Later refinements of this technique, reported by W. T. Sproule (4), permitted individual determinations of stress without prior knowledge of the stress free "d" spacing. This improved method, known as the "two exposure method" is the fundamental procedure in most X-Ray stress studies today.

Let us then consider this fundamental principle in more detail. Given: a specimen whose surface is represented by many randomly oriented grains, some with planes parallel to the surface, others

30°, 55°, 69°, 90°, etc. (Figure 2).

Let us further confine our investigation to the grains with planes parallel and 30° to the surface. First, a determination is made of the "d" value of the planes parallel to the surface, parallel to direction of stress (Figure 2A). Then a second exposure is made at an angle 30° to the surface and direction of stress (Figure 2B). Both these measurements were obtained following the principles in Figure 1.

If the stress is tension, the interplanar spacing "d_⊥" in Figure 2A will be shortened. In Figure 2B, however, the interplanar distance "d_ψ" has not been affected as much by the stress, but by a lesser amount and a function of the angle ψ (30°). "d_ψ" then will be slightly greater than "d_⊥", but what is more important, it gives us the rate at which the stress is affecting the interplanar distances with changes in "ψ" angles. Consequently, a rate ratio,

$$\frac{d_{\psi} - d_{\perp}}{d_{\perp}}$$

can be set up to determine stress directly from the equation:

$$s = \frac{d_{\psi} - d_{\perp}}{d_{\perp}} \times \frac{E}{1 - u} \times \frac{l}{\sin^2 \psi} \quad (\text{Equation 2}),$$

where E = Young's Modulus, u = Poisson's ratio. The theory and derivation for this equation can be found in reference (5) by C. S. Barrett, page 322.

When applying these principles to the measurement of stress, most investigators agree that it is permissible, in general, to use the mechanical values of the elastic constants without correction for the anisotropy known to exist in iron. They reasoned that, although little is known of anisotropic crystals at a given orientation with respect

to a certain stress, possibly the whole mass would be governed by random orientation and would behave isotropically in the absence of preferred orientation. From a practical viewpoint then, successful X-Ray measurements of stress can be made considering the specimen as an isotropic whole.

For a more comprehensive discussion of the fundamentals of X-Ray diffraction, the reader is referred to the several treatises in the Bibliography.

TECHNIQUE

The essential elements of an X-Ray diffraction spectrometer consist of a source of X-Rays, a sample holder, and a Geiger pick-up counter (or photographic plate) to record the X-Rays reflected from the sample. In figure 3 is pictured a "General Electric Corporation XRD-3 X-Ray Spectrometer" with a horizontal direct measurement spectrogoniometer of radius 5.73 inches.

At the end of the Coolidge X-Ray tube is a chromium target on line with the Geiger counter and sample when the Geiger counter is in a zero 2θ position angle. The choice of a chromium target was based upon the need to have a radiation of longer wave length than the characteristic radiation of the material under examination. The softness of the chromium radiation also contributes to the line sharpness which is a valuable consideration in the case of strain measurements on steels.

For every degree of 2θ the Geiger counter moves on the goniometer circle (with degree markings, Figure 3) the sample, through a gear mechanism moves only half a degree of θ . This is necessary to maintain a focusing condition for all angles of 2θ .

Accurate integration of the X-Ray intensity reflected from the sample is accomplished by electronically counting the number of pulses emitted by the Geiger counter and recording the time required to obtain a pre-selected number of these pulses. Recording time, the inverse measure of intensity, is advantageous over counting the pulses directly in that the probable error can be kept constant.

Once the proper choice of filters and slits is assembled and the unit activated, a graphic record of the diffraction pattern is recorded as the Geiger counter automatically scans through 160° , 2θ

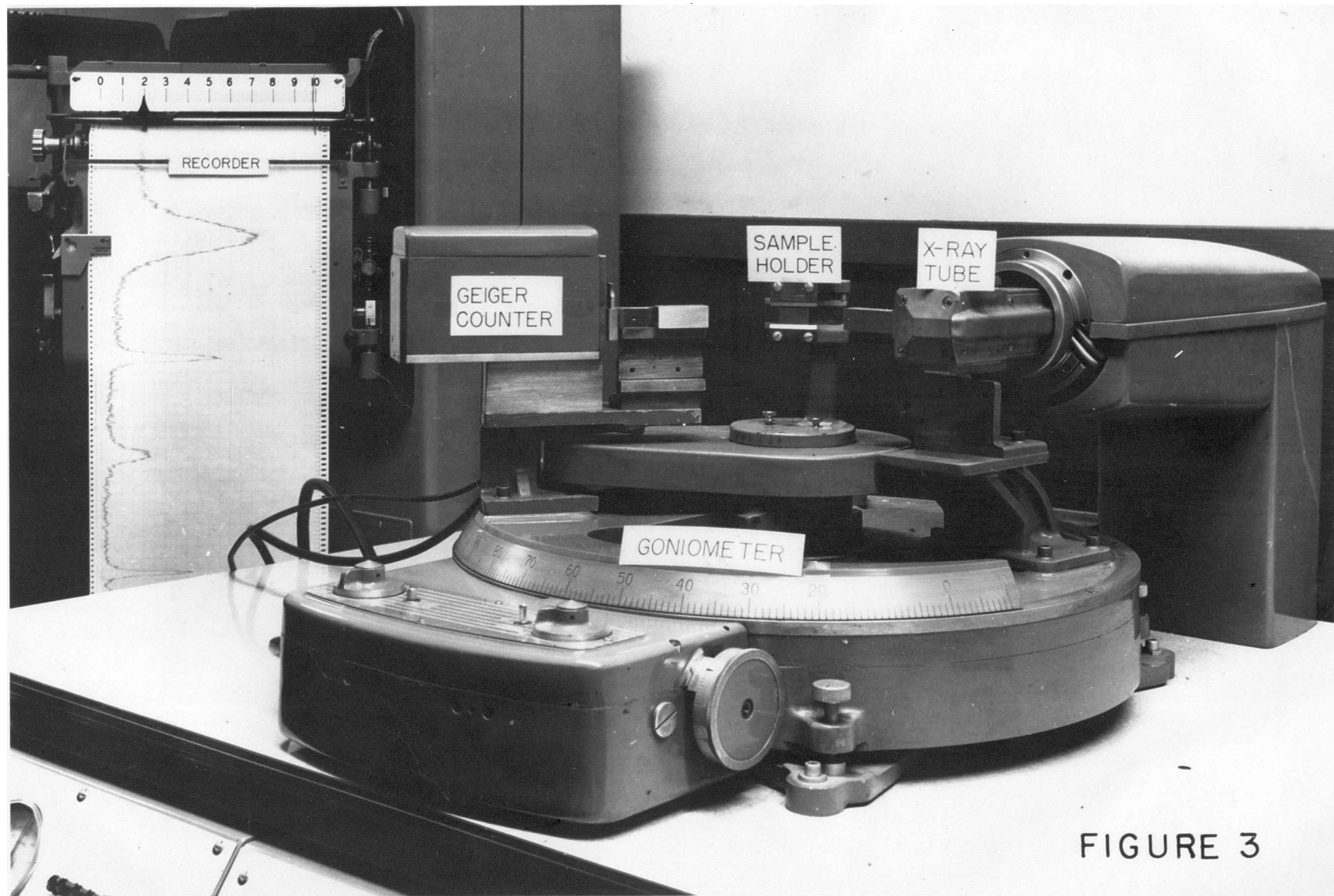


FIGURE 3

(Figure 4). The appearance of a peak indicates an increase of reflected intensity from a series of parallel crystal planes having the same Miller indices, or a multiple of them as in Figure 1. An analogy might be drawn from a beam of light striking the faces of a multi-cut diamond as the light is rotated twice as fast as the diamond.

Especially suited to the measurement of small changes in the interplanar distance "d" is the back reflection region or to the extreme left on Figure 4, above 130° . It is for this trigonometric reason that the highest possible angle of 2θ is recommended where a strong, well defined peak appears. In the case of hardened steels the peak at about 156° has been identified as the (211) martensite line. The author has confined his investigation to this peak in analyzing for strain changes and temperature effects.

Figure 5 graphically illustrates the technique in measuring the peak angle. By determining two or more points along the straight line portion of both sides of the peak, the corrected peak angle is calculated by solving for the intercept of these straight line equations. A shift towards $0^{\circ} 2\theta$ means an increase in "d" spacing, and conversely, a shift towards $180^{\circ}, 2\theta$, means a decrease in "d" spacing. As mentioned above, a tension stress accompanies a decrease in "d" value and compression an increase.

Peak movement is brought about by the "macro" and "micro" stresses, whereas peak broadening is due only to the "micro" stress. The illustration in Figure 5 is a highly micro-stressed specimen and also contains macro stresses, but which won't be apparent until the shift in peak is determined by the two exposure method.

Micro-strains may be defined as "strains that have been set up

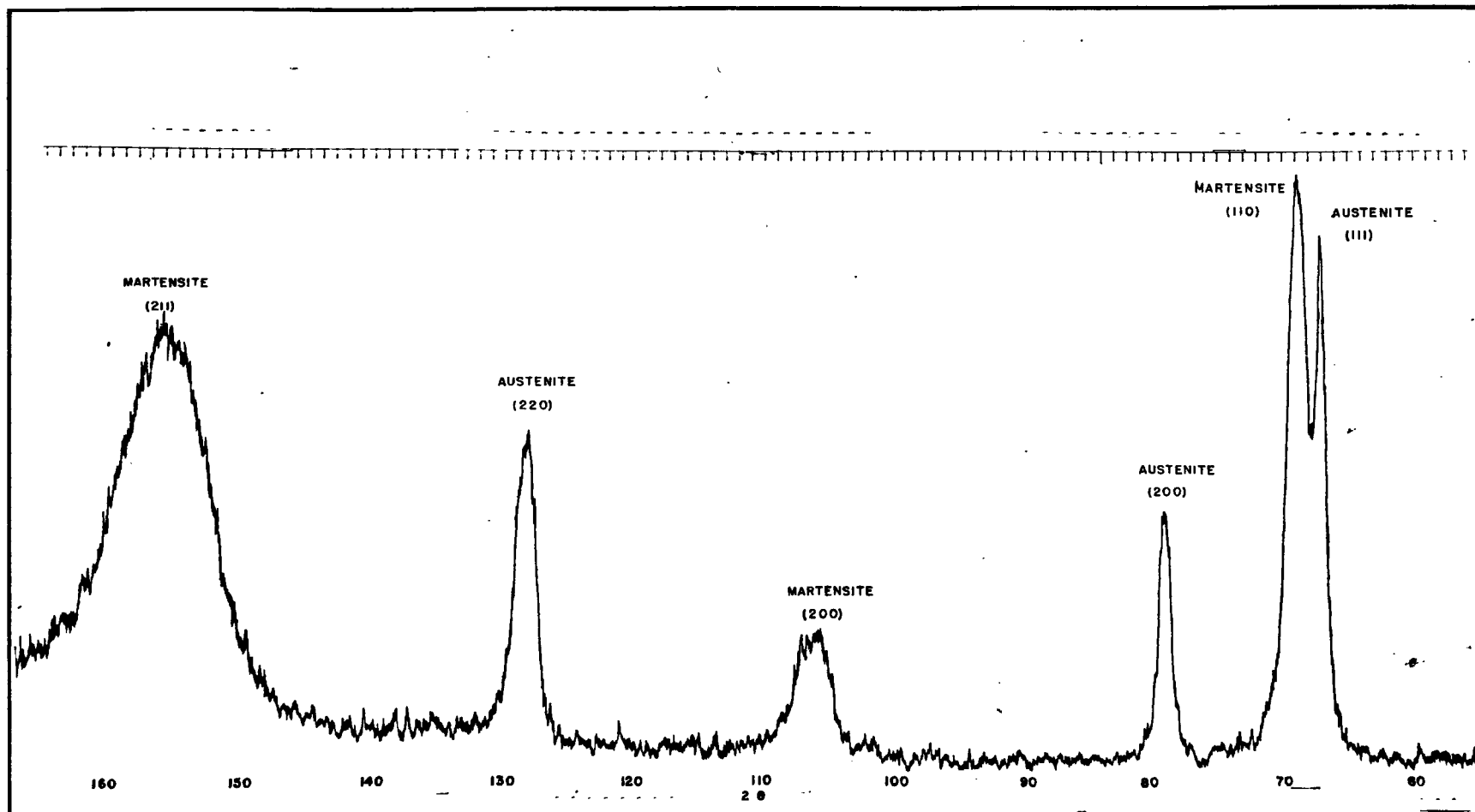


FIGURE 4

by the accompanying phase transformations and are usually distributed through microscopic volumes." Residual strains caused by differential plastic flow, as in cold working, are usually distributed through appreciable volumes and are referred to as "macrostressess".

Equipped with this tool, accurate studies can be made of the macrostructural properties of polycrystalline metals as they are influenced from the surrounding conditions. The full importance and advantages of this technique have not as yet been realized, due in part to some limitations still to be eliminated. Only with the cooperation of the various research laboratories now undertaking this study will the technique be improved to where industry can fully benefit from this new discovery.

EXPERIMENTAL PROCEDURE

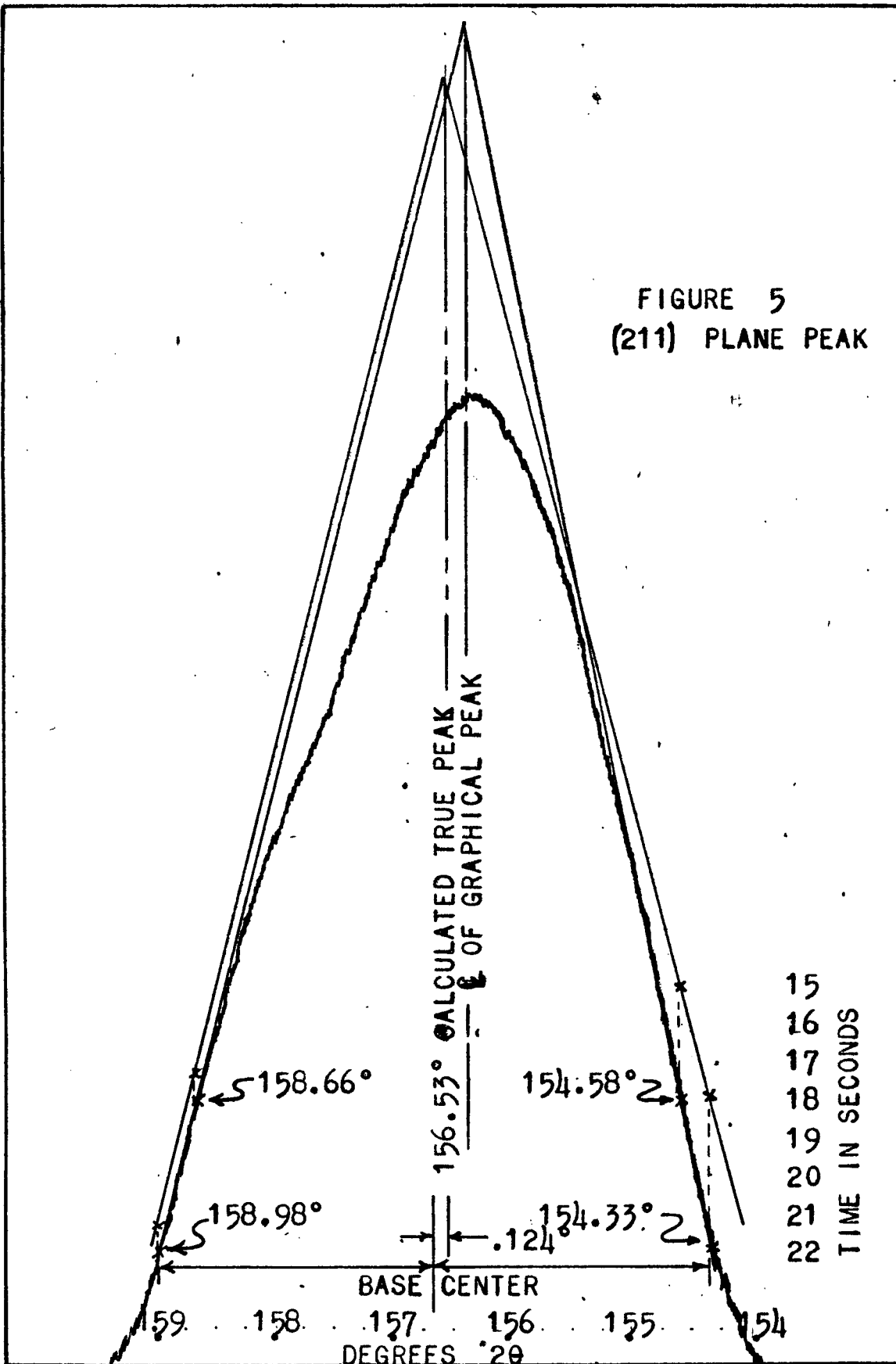
In light of the adolescence of X-Ray diffraction and the many unknowns to be solved, the author has undertaken first, a study of some specific questions relative to the measurement of strain, and second a comparison of the effects of the lattice dimensions and the linear thermal expansion coefficients of carburized Vs. non-carburized low alloy steels.

With the development of a technique for measuring stress in hardened steels by A. L. Christenson and E. S. Rowland (6), higher stresses could be measured with the same accuracies obtained as when measuring the lower stresses. Percentage-wise, this meant an increase in precision where larger stress values were to be determined. This method was further improved by the author by choosing two points out of the several along each "straight" side that were most nearly linear (Figure 5).

Most of Christenson's data was obtained using a shift in ψ angle of 45° and 60° for accuracy in computations at the sacrifice of accuracy from intensity. All strain investigations covered in this paper, however, were made using a ψ angle of 30° to obtain greater accuracy through increased intensity.

The reader is directed to the sample calculations in the Appendix for an explanation of how the corrected peak is obtained. The "d" spacing in Angstrom units can be found in the standard (chromium radiation) table for converting diffraction angles to "d" dimensions. The change in "d" from 0° to $30^\circ \psi$ multiplied by a constant of proportionality factor of 8000 psi obtained from Equation 2, measures

FIGURE 5
(211) PLANE PEAK



the surface stress in the horizontal plane of the sample (Figure 9).

Sample surface preparation was most adequately solved by electro-etching in a 10% bath of sulfuric acid. The removal of one or two thousandths was found to be sufficient.

First Investigation: Relative to the Measurement of Stress -
"Preferred Orientation of Grinding Stresses".

It is usually recognized that grinding induces residual tension stresses in the surface of steels. In his article on "Residual Stress Measurements", D. G. Richards (7) suggests that the amount of stress induced depends on the prior metallurgical history of the specimen and the extent of grinding; that the stress mechanism results from the thermal action of the heat of grinding.

Although structural changes could cause induced tension stress, since, in this case, the piece was tempered at 1000 - 1100^oF, it is rather to be expected that the stresses were induced by upsetting the surface caused from the thermal expansion while the sub-surface remained cold. Actually, a .002 of an inch pass over the specimen left an evenly discolored surface. The evidence of so much local heat below the tempering temperature tends to substantiate the theory of "Thermal Upsetting".

The X-Ray technique measures strains in the surface of the specimen coplanar with the direction of the stress being determined. This means that the stress component in one direction is measured correctly, regardless of whether there is a component normal to it or not. This was clearly demonstrated by grinding a specimen of "18-4-1" tool steel heat treated and tempered to a hardness of 45 Rockwell "C". An evenly distributed 67,000 psi compressive stress existed before the

grind. Figure 7 shows the distribution of stress after grinding with a preference in the direction. These values represent an average of 3 independent strain determinations. (See data Table I in the Appendix).

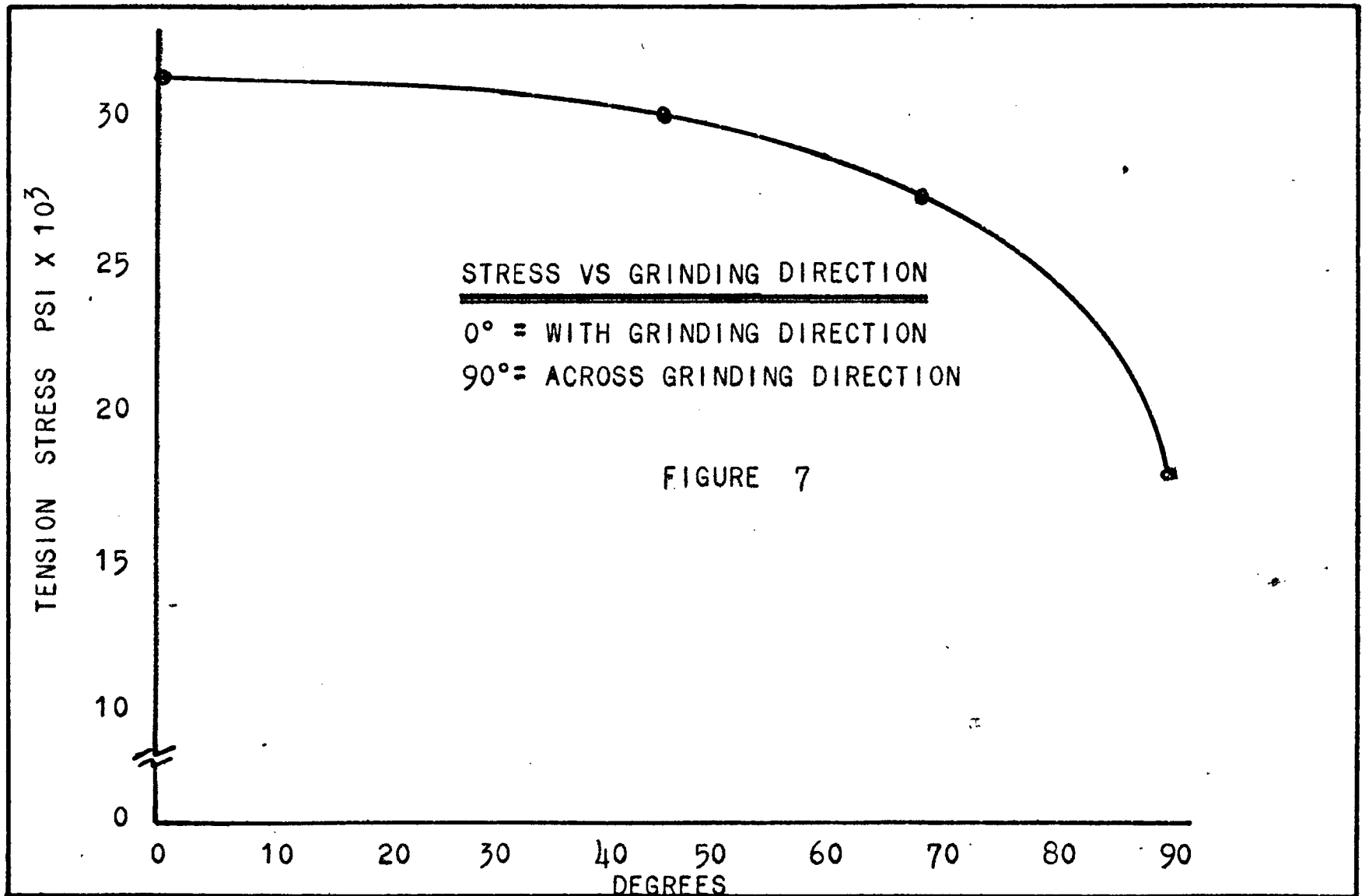
From 67,000 psi compression to 31,000 psi tension represents an induced stress of 98,000 psi due to grinding, while normal to the ground direction, the stress measured only 85,000 psi. Intermediate measurements were made at 45° and $67\frac{1}{2}^{\circ}$ which followed the stress progression.

The high induced tension stress developed by grinding was found to definitely exhibit some preferred orientation, although the attempt to chart a pole figure diagram of the stress distribution proved inconclusive. The low stress differential after grinding and the fine grain size probably prevented any clear orientation study. This investigation on grinding is compared to the effects from extruding a mild steel bar for a final analysis. A brief description of the "pole figure" plotting procedure is given after the discussion on extruding.

Second Investigation Relative to the Measurement of Stress -

"Preferred Orientation of Stresses from Extrusion".

To examine the principles of preferred orientation further, a piece of AISI 1020 cold roller strip was studied for the effects of rolling on the orientation of residual stress. After determining a low stress of 6000 psi tension, however, the piece was thought not to be a good example. It was decided then to apply a known amount of plastic deformation so a definite orientation would be established. With this in mind, a piece of hot rolled strip with an average isotropic stress of 6000 psi compression was extruded and reduced 44% in 3 passes through two semi-stationary rollers.



The purpose of a hot rolled sample here was two-fold; first, the residual stress would be almost zero, and second, what stresses did exist would be equal or nearly so in all directions.

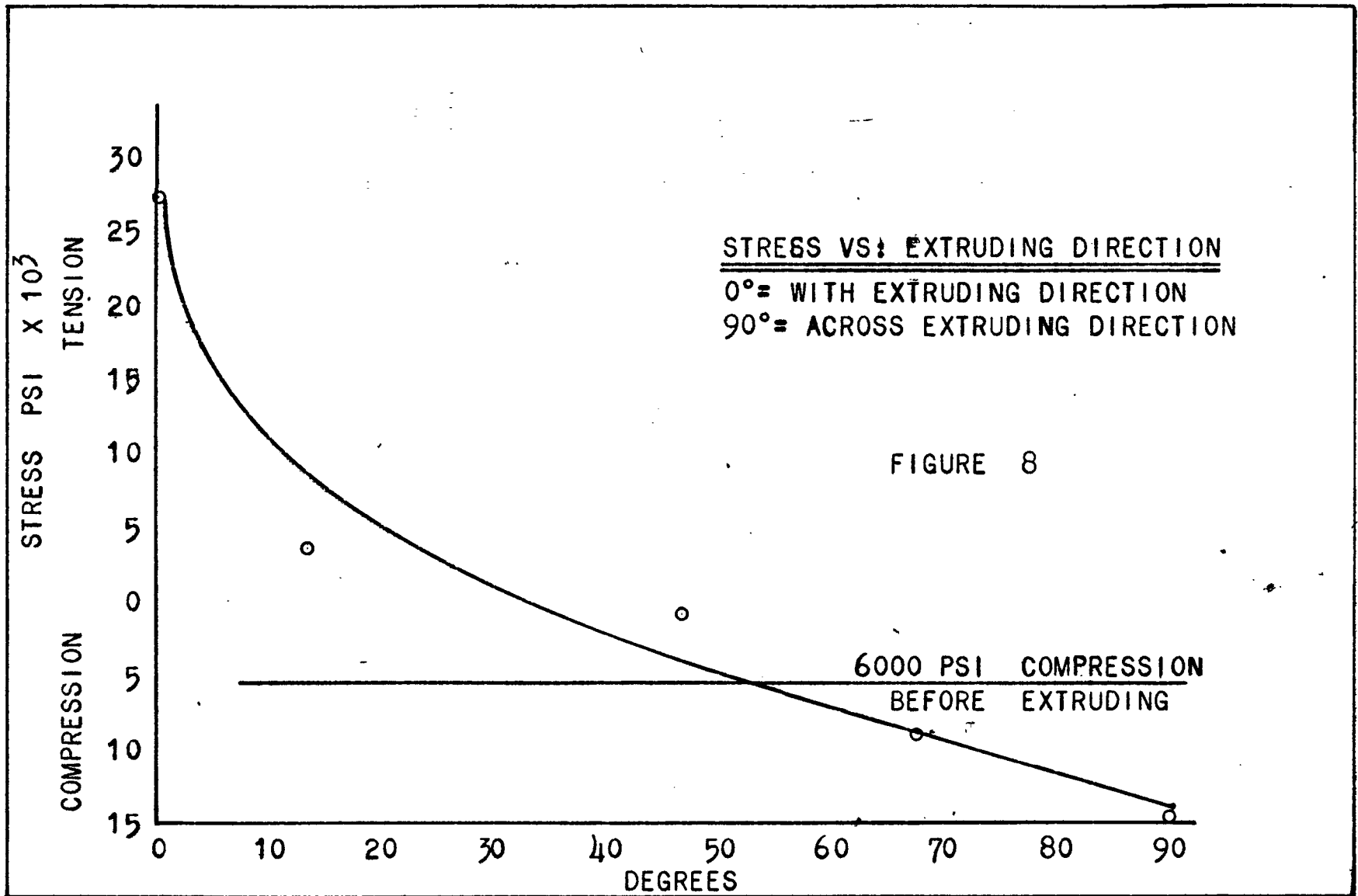
The results of the stress distribution as determined by X-Ray diffraction are tabulated on test data Table II (see Appendix) and are graphically shown in Figure 8. Strains of considerable magnitude were induced from plastically deforming the grains by extruding.

Using, from the curve, the maximum compression stress developed (-6000 to -14,500 = -8500 psi) and relating this to the maximum tension stress developed (-6000 to ~~+27,000~~ = ~~+33,000~~ psi) a very close approximation was found to Poisson's ratio:

$$\frac{8500}{33,000} = .26 \text{ (Poisson's ratio for iron = .28).}$$

This should not be surprising since the ratio of traverse contraction of a strained test specimen to its longitudinal elongation is Poisson's ratio. In this case, the contraction (compression) was 8500 psi, and the elongation (tension) was 33,000 psi.

There was no doubt of the existence of preferred orientation since the longitudinal elongation was positively established. Due to the inflexibility of the XRD-3 unit to measure orientation, the attempt at charting a "pole figure" was sketchy and not too accurate. However, it is enclosed as Figure 6 for information. The procedure for making a "pole figure chart" can be found in accurate detail in Reference (8) in the Bibliography. Briefly, the sample is rotated 360° , in 15° increments, about an axis normal to its surface. The build up of intensity is recorded by a suitable numbering system on a graphical chart, one type of which is shown in Figure 6. The larger numbers representing higher intensities appear every 90° and indicate a pre-



ferred orientation. A pole figure representation of a specimen provides the most complete picture of the crystal orientation.

This evidence substantiates the information given on the grinding studies reported earlier. No pole figure could have been made because very little elongation had taken place. The high stresses developed were definitely caused by the thermal effects from the heat generated by grinding.

Third Investigation Relating to the Measurement of Stress - "Effects of Temperature".

From the Laws of the Physics of Metals it is known that steel (iron) contracts on cooling and expands with heating. The linear coefficient of thermal expansion of iron near 68°F is 6.5×10^{-6} inches per inch per degree Fahrenheit (°F) as determined by dilatometric methods. The usual procedure uses a pure rod of the metal under study, 300 mm long, which unavoidably has randomly oriented crystals. An average coefficient is thus established for expansion in every crystallographic direction.

Here again is an example where X-Ray diffraction techniques can improve on past methods. Not only can thermal expansion coefficients be determined by X-Ray procedures, but the coefficients can be individually measured in any crystal plane direction. For correlation with the average coefficient as determined by the dilatometric method, the change in the interplanar distance "d" between the (211) planes was found to represent this average value closely.

The thermal expansion coefficient can accordingly be written 6.5×10^{-6} Angstroms per Angstrom per degree Fahrenheit. In the calculation of stress, every 10^{-7} Angstrom unit difference in "d" spacing is multi-

plied by 8 pounds per square inch (from Equation 2). One degree change in temperature equals 6.5×10^{-7} Angstrom units change in "d" spacing, which when multiplied by 8 represents 520 psi stress, or 5200 psi for ten degree change.

This may or may not seem to be much of an influence "per se", but multiplied several times by the complexity of the calculations, it could be a hazardous factor. Conversely, in many cases, these temperature errors could be self compensating. The importance of maintaining constant temperature conditions cannot be over-emphasized, especially when working with small samples over extended periods of time.

Fourth Investigation - "Comparisons of Structures and Thermal Expansion Coefficients of 'Straight' Carbon Steels, Carburized and Non-Carburized".

An attempt was made to correlate the effects on the atomic structure within the grains of a plain carbon steel to a similar piece of steel carburized to the same carbon level, as a function of the carbon content. It was thought, in either steel, that as the carbon percentages were changed the lattice dimensions and thermal expansion coefficient would be affected proportionately.

With this in mind, several analyses of the hot rolled "straight carbon steel" variety were obtained over a range of carbon content (see test data Table III in Appendix). After a suitable electropolish and etch the "d" values of samples 1 through 6 were determined. Before measurements were made all samples were salt bath annealed to equalize possible differences in microstructure.

An evaluation of the data showed no statistical relationship to exist between the "d" spacing and the substitutional carbon content in

the carbon range studied. Variations in manganese contents might have influenced the values, but no direct correlation was evident from the data.

These same steel samples were examined for their thermal expansion coefficient between 100° and 200°F. A simple ratio between the "d" spacings at the two temperatures gives this as follows:

$$\frac{d_{200} - d_{100}}{d_{100}} \times \frac{1}{t_2 - t_1} = \text{Expansion coefficient}$$

or,

$$\frac{1.1707818 - 1.1700353}{1.1700353} \times \frac{1}{200-100} = 6.38 \times 10^{-6} \text{A}^\circ/\text{A}^\circ/\text{F}^\circ$$

Figure 9 shows the XRD-3 unit set up for measuring the change of 2θ with temperature increase. The galvanometer on the left measures the millivolts generated through the thermocouple silver-soldered to the back of the sample which is enclosed in the insulated box, now cut away for the purpose of viewing the sample and holder inside. The portable hot air blower behind the galvanometer supplies the heat to the sample. It is regulated by the powerstat located to the right of the goniometer circle. The temperature can be controlled and measured to $\pm 1/2^\circ\text{F}$ without difficulty.

Again, the data provided no consistent values to relate the expansion coefficients with carbon content. It can only be assumed then that substitutional carbon additions do not affect these two physical properties of steel in the carbon range examined.

The second part of this investigation dealt with carburized (interstitial carbon) AISI 1020 steel with carbon percentages approximating that of the steels used above. The manganese content remained constant in this case, all samples being from the same steel.

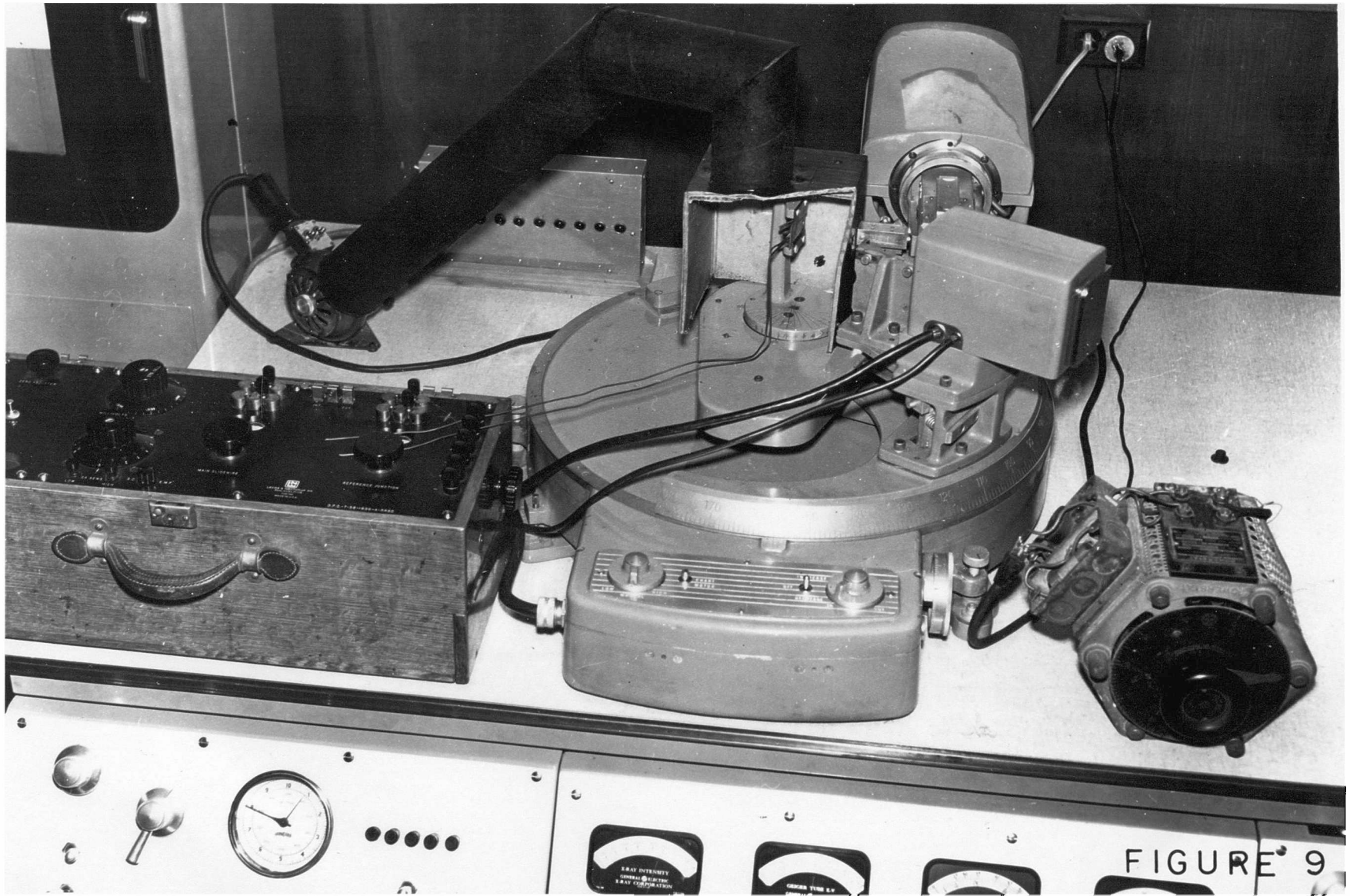


FIGURE 9

A Leeds and Northrup "Homo-Carb" furnace with "Micro-Carb" control was used to carburize the 1/8" thick samples to various carbon levels. Several attempts to control carbon input proved futile until a load of scrap was run along with the samples. Two samples were run together, one for the test piece and the other for the chemical analysis. All samples were salt bath annealed. A comparison was also made of the microstructures to verify the chemical analysis and annealing treatment. The "d" values and expansion coefficients were determined as before and recorded on the test data sheet.

The interpretations were again difficult and inconclusive. In the carbon range which was obtained from the "Homo-Carb", no trend was evident in either the interplanar distances or the thermal expansion coefficients. However, the overall observation of carburized to non-carburized revealed quite plainly the larger values of "d" spacing and higher coefficients of thermal expansion in the carburized steels. This would concur with the commonly accepted belief that the volume and density would increase with carburization.

SUMMARY AND CONCLUSIONS

Although an appreciable change in stress occurred, very little preferred orientation was established from the effects of heavy grinding. The stress change was brought about by the upsetting of the surface caused by thermal expansion, from the heat of grinding and not from plastic deformation. The slight preference in the direction of grinding was induced by a cold working effect analogous to a machining operation.

The extruding tests set up a positive preferred orientation condition. Accurate studies of preferred orientation of stress can be made using the method of strain measurements. The accuracy was substantiated by the close agreement to Poisson's ratio through a comparison of the distribution of induced stresses.

The XRD-3 X-Ray unit proved to be so sensitive that for accurate strain studies temperature control is mandatory. A single degree change at a crucial point could greatly affect the final stress value.

The study of the carburized and uncarburized straight carbon steel as a function of their carbon content provided very little information from the effects on the lattice dimensions and thermal linear expansion coefficients. However, these properties in the carburized steels were on an average larger than the uncarburized values.

It is hoped and expected that through the combined efforts of all interested in the X-Ray study of the behavior of metals, a working technique will be developed to put these measurements and many more on a routine laboratory basis. It is further hoped that the reader, through this and other reports will better understand the possibilities of this method of analysis.

BIBLIOGRAPHY

1. Lyman, Taylor (Editor), Metals Handbook, Cleveland, Ohio, American Society for Metals, 1948.
2. Lester, H. H. and Aborn, R. H., Army Ordnance, 6, 1925-26.
3. Sachs, G. and Weertz, J., Z. Physik Vol. 64, 481, 1930.
4. Sproule, W. T., X-Rays In Practice, New York: McGraw-Hill Book Company, 1945.
5. Barrett, C. S., Structure of Metals, New York: McGraw-Hill Book Company, 1943.
6. Christenson, A. L. and Rowland, E. S., "X-Ray Measurement of Residual Stress in Hardened High Carbon Steel", Vol. 45 of Transactions of American Society for Metals, Cleveland, Ohio, American Society for Metals, 1953.
7. Richards, D. F., "Relief and Distribution of Residual Stress in Metals", Residual Stress Measurements, Cleveland, Ohio, American Society for Metals, 1951.
8. Klug, H. P. and Alexander, L. E., X-Ray Diffraction Procedures, New York: John Wiley and Sons, Inc., 1954.
9. Norton, J. T., "X-Ray Methods in the Field of Residual Stress", Vol. 2, No. 1 of Proceedings of the Society for Experimental Stress Analysis, New York: John Wiley and Sons, Inc., 1944.

APPENDIX

SAMPLE CALCULATIONS

In figure 5 two points on each side of the peak were plotted as lying on the straight line portion of the curve. Since this curve is distorted by the unequal background and the Ka radiation doublet effect, solving the equations of these two sides will not give the correct peak angle. A correction to the slopes must be applied to compensate for the distortion. In Step 1 the original data was tabulated and the uncorrected slopes determined.

Step 1

<u>2 θ</u>	<u>Inverse Intensity (Time in Seconds)</u>	<u>2 θ</u>	<u>Inverse Intensity (Time in Seconds)</u>
154.58	18	158.98	22
<u>154.33</u>	<u>22</u>	<u>158.66</u>	<u>18</u>
.25	<u>4</u>	.32	<u>4</u>

$$\text{Slope} = \frac{4}{.25} = 16 \text{ sec/degree}$$

$$\text{Slope} = \frac{4}{.32} = 12.5 \text{ sec/degree}$$

It is apparent that these slopes are not equal and must be adjusted to make the peak curve symmetrical, for only with symmetry will the lines be on the same intensity basis.

The value 0.02 second per degree was arbitrarily taken and applied to the ($160^{\circ} - 2\theta$) readings (Step 2) and subtracted from one. The multiplication factors, assumed to be one at 160° were then applied to the four original values of intensity (Step 3).

Step 2

<u>2 θ</u>	<u>(160 - 2 θ) .02</u>	<u>Multiplication Factors</u>
154.33	(160 - 154.33) .02 = .1134	1 - .1134 = .8866
154.58	(160 - 154.58) .02 = .1084	1 - .1084 = .8916
158.66	(160 - 158.66) .02 = .0268	1 - .0268 = .9732
158.98	(160 - 158.98) .02 = .0204	1 - .0204 = .9796

Step 3

<u>2 θ</u>	<u>Inverse Intensity X Correction (Time in Seconds) Factor</u>	=	<u>Corrected Intensity</u>
154.33	22 X .8866	=	19.5052
154.58	18 X .8916	=	16.0488
158.66	18 X .9732	=	17.5176
158.98	22 X .9796	=	21.5512

Subtracting intensities and dividing by the difference in 2 θ value as in Step 1, the relative slopes from these corrected intensities were again determined and found to be 13.8256 and 12.6050 seconds per degree, respectively.

It is observed that more correction will be necessary. However, since the change in slope on each side of the peak induced by the correction is essentially a linear function, a rate of change can be established into two linear equations. Equating and solving simultaneously, these equations yield the true increase per degree of correction factors necessary to equalize the slopes (Step 4). Using this true increase per degree, the correction factors were computed (Step 5). From this, the corrected intensities and equal slopes were tabulated (Step 6).

$$\underline{\text{Step 4}} \quad 16.0 - \frac{(16.0 - 13.8256) x}{.02} = 12.5 - \frac{(12.5 - 12.6050) x}{.02}$$

$$16.0 - 12.5 = 5.25 x \quad \neq 108.72 x$$

$$x = .02071$$

Step 5

<u>2 θ</u>	<u>(160 - 2 θ) .02071</u>	<u>Correction Factor at 2 θ</u>
154.33	(160 - 154.33) .03071 = .17412	1 - .17412 = .82588
154.58	(160 - 154.58) .03071 = .16645	1 - .16645 = .83355
158.66	(160 - 158.66) .03071 = .04115	1 - .04115 = .95885
158.98	(160 - 158.98) .03071 = .03132	1 - .03132 = .96868

Step 6

<u>2 θ</u>	<u>Inverse Intensity</u> <u>(Time in Seconds) X</u>	<u>Correction</u> <u>Factor</u>	=	<u>Corrected</u> <u>Intensity</u>
154.33	22 X	.82588	=	18.16936
154.58	18 X	.83355	=	15.00390
158.66	18 X	.95885	=	17.25930
158.98	22 X	.06868	=	21.31096

154.33	18.16936	158.98	21.31096
154.58	<u>15.00390</u>	158.66	<u>17.25930</u>
	3.16546		4.05166

$$\text{Slopes: } \frac{3.16546}{.25} = \underline{\underline{12.661}} \qquad \frac{4.05166}{.32} = \underline{\underline{12.661}}$$

With the slopes equal, the correction for the "tilt" of the curve can be computed in degrees. This is then subtracted from the base center of the uncorrected peak.

$$\begin{array}{r} 158.98 \quad 21.31096 \\ 154.33 \quad \underline{18.16936} \\ \quad \quad \underline{3.14160} \end{array} \qquad \frac{3.14160}{12.661} = .248 \div 2 = .124^\circ \text{ correction}$$

$$\begin{array}{r} 156.655 \\ \underline{.124} \\ 156.531^\circ \text{ (Corrected Peak at } 0^\circ \psi) \end{array}$$

The same procedure was followed for $30^\circ \psi$ from which a value of 156.37° was calculated.

The difference in the "d" values of these angles multiplied by the stress factor 8×10^7 psi (from Equation 2) determines the stress.

$$\begin{array}{r} \psi \\ 30^\circ \\ 0^\circ \end{array} \qquad \begin{array}{r} 2 \theta \\ 156.370 \\ 156.531 \end{array} \qquad \begin{array}{r} \text{"d"} \\ 1.1694936 \\ 1.1691560 \\ \underline{.0003376} \times 8 \times 10^7 = 27,000 \text{ psi} \\ \text{(tension)} \end{array}$$

TEST DATA TABLE I
DISTRIBUTION OF GRINDING STRESSES

Angle to Grinding Direction	Test No	d 30° (A°)	d 0° (A°)	(d ₀ - d ₃₀) or (d ₃₀ - d ₀)	Stress (psi)	Average of 3(psi)
0°	1	1.1711311	1.1707316	.0003995	31,960	
	2	1.1711289	1.1707338	.0003951	31,608	31,035 (T)
	3	1.1711245	1.1707490	.0003755	30,040	
45°	1	1.1711775	1.1707913	.0003862	30,896	
	2	1.1711642	1.1708037	.0003605	28,840	30,000 (T)
	3	1.1711488	1.1707705	.0003783	30,264	
67°	1	1.1712084	1.1708672	.0003412	27,296	
	2	1.1712022	1.1708708	.0003314	26,512	27,261 (T)
	3	1.1712125	1.1708628	.0003497	27,976	
90°	1	1.1711215	1.1709462	.0001753	14,024	
	2	1.1711357	1.1708935	.0002422	19,376	18,000 (T)
	3	1.1711444	1.1708869	.0002575	20,600	
BEFORE GRINDING						
	1	1.1717797	1.1726162	.0008365	66,920	
	2	1.1718016	1.1726208	.0008192	65,536	66,620 (C)
	3	1.1718263	1.1726690	.0008427	67,416	

TEST DATA TABLE II
DISTRIBUTION OF EXTRUDING STRESSES

Direction	Test No	d 30° (A°)	d 0° (A°)	(d ₀ - d ₃₀) or (d ₃₀ - d ₀)	Stress (psi)	Average of 3(psi)
0°	1	1.1694936	1.1691560	.0003376	27,008	
	2	1.1694886	1.1691633	.0003253	26,024	26,996 (T)
	3	1.1695021	1.1691539	.0003482	27,856	
15°	1	1.1693233	1.1692875	.0000358	2,864	
	2	1.1693128	1.1692785	.0000343	2,744	2,909 (T)
	3	1.1693380	1.1692990	.0000390	3,120	
45°	1	1.1693055	1.1693223	.0000168	1,344(C)	
	2	1.1693002	1.1693420	.0000418	3,344(C)	950 (C)
	3	1.1693170	1.1692940	.0000230	1,840(T)	
67½°	1	1.1692620	1.1693821	.0001201	9,608	
	2	1.1692542	1.1693884	.0001342	10,736	8,970 (C)
	3	1.1692709	1.1693506	.0000797	6,376	
90°	1	1.1692514	1.1694336	.0001822	14,576	
	2	1.1692559	1.1694410	.0001851	14,808	14,530 (C)
	3	1.1692458	1.1694234	.0001776	14,208	

BEFORE EXTRUDING

As Rec'd.	1	1.1692052	1.1692894	.0000842	6,736	
Hot	2	1.1692020	1.1692825	.0000805	6,440	6,146 (C)
Rolled	3	1.1692115	1.1692774	.0000659	5,272	

TEST DATA TABLE III
ANALYSES AND PHYSICAL CONSTANTS

Test No.	AISI Spec.	Carbon (%)	Mang. (%)	do* (A°)	Thermal Expansion Coefficient x 10 ⁻⁶ A°/A°/F° **
1	1095	.95	.50	1.1700353	6.38
2	1082	.87	.78	1.1701641	6.12
3	1070	.73	.81	1.1701318	6.67
4	1055	.57	.67	1.1698964	6.63
5	1030	.24	.39	1.1701318	6.67
6	1015	.12	.58	1.1703904	6.88

CARBURIZED

A	1020	1.18	.54	1.1704337	6.35
B	"	.92	.52	1.1704987	6.75
C	"	.78	.53	1.1703904	7.47
D	"	.64	.50	1.1703040	7.10
E	"	.43	.52	1.1704229	6.82

* At 100° F

** Between 100 and 200° F

TABLE IV

POLE FIGURE DATA TABLE FOR 44% EXTRUDED "1020" STEEL

ROTATION OF SAMPLE	ROTATION OF SAMPLE HOLDER (α°)													
	0°		10°		20°		30°		40°		50°		60°	
	*	**												
	INTENSITY	#	INTENSITY	#	INTENSITY	#	INTENSITY	#	INTENSITY	#	INTENSITY	#	INTENSITY	#
15°	6.00	1	5.65	1	5.90	2	5.90	3	5.55	2	5.85	3	5.70	3
30°	5.95	1	5.70	1	5.70	1	5.80	2	5.55	2	5.65	2	5.50	2
45°	6.00	1	5.75	1	5.70	1	5.70	1	5.60	2	5.55	1	5.40	1
60°	6.05	2	5.80	1	5.75	1	5.65	1	5.50	1	5.50	1	5.40	1
75°	6.05	2	6.00	2	5.90	2	5.70	1	5.50	1	5.50	1	5.45	1
90°	6.15	3	6.20	3	6.20	3	5.90	3	5.70	3	5.65	2	5.45	1

(REPETITIOUS FOR EACH QUADRANT)

* Intensity measured by linear height on recorded graph.

** Relative number given to intensity value.

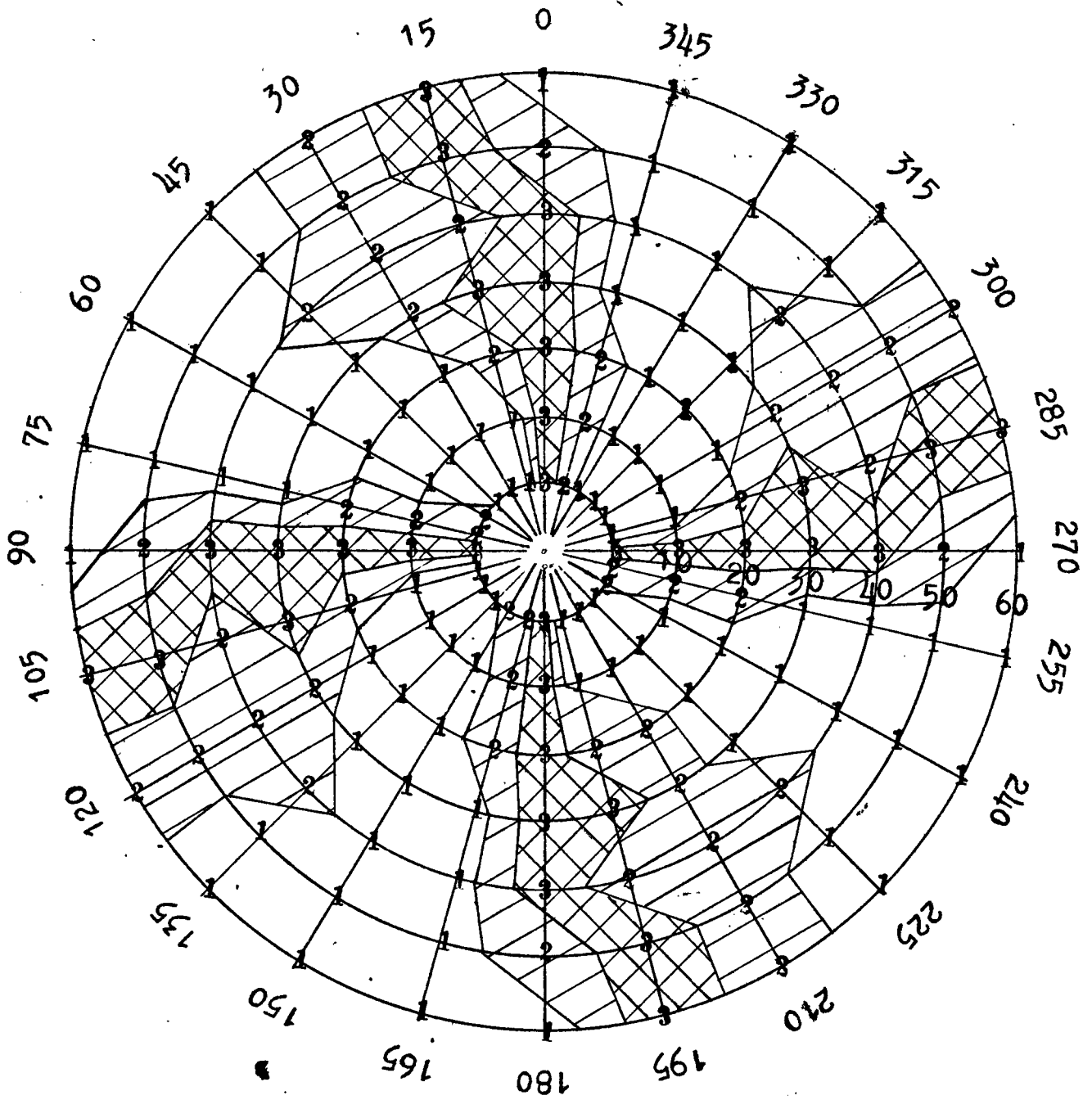


FIGURE 6
 POLE FIGURE DIAGRAM INDICATES
 MAXIMUM ORIENTATION EVERY 90°